

## LETTERS

# Cyclic dermal BMP signalling regulates stem cell activation during hair regeneration

Maksim V. Plikus<sup>1</sup>, Julie Ann Mayer<sup>1</sup>, Damon de la Cruz<sup>1</sup>, Ruth E. Baker<sup>2</sup>, Philip K. Maini<sup>2,3</sup>, Robert Maxson<sup>4</sup> & Cheng-Ming Chuong<sup>1</sup>

In the age of stem cell engineering it is critical to understand how stem cell activity is regulated during regeneration. Hairs are mini-organs that undergo cyclic regeneration throughout adult life<sup>1</sup>, and are an important model for organ regeneration. Hair stem cells located in the follicle bulge<sup>2</sup> are regulated by the surrounding microenvironment, or niche<sup>3</sup>. The activation of such stem cells is cyclic, involving periodic  $\beta$ -catenin activity<sup>4–7</sup>. In the adult mouse, regeneration occurs in waves in a follicle population, implying coordination among adjacent follicles and the extrafollicular environment. Here we show that unexpected periodic expression of bone morphogenetic protein 2 (*Bmp2*) and *Bmp4* in the dermis regulates this process. This BMP cycle is out of phase with the WNT/ $\beta$ -catenin cycle, thus dividing the conventional telogen into new functional phases: one refractory and the other competent for hair regeneration, characterized by high and low BMP signalling, respectively. Overexpression of noggin, a BMP antagonist, in mouse skin resulted in a markedly shortened refractory phase and faster propagation of the regenerative wave. Transplantation of skin from this mutant onto a wild-type host showed that follicles in donor and host can affect their cycling behaviours mutually, with the outcome depending on the equilibrium of BMP activity in the dermis. Administration of BMP4 protein caused the competent region to become refractory. These results show that BMPs may be the long-sought ‘chalone’ inhibitors of hair growth postulated by classical experiments. Taken together, results presented in this study provide an example of hierarchical regulation of local organ stem cell homeostasis by the inter-organ macro-environment. The expression of *Bmp2* in subcutaneous adipocytes indicates physiological integration between these two thermoregulatory organs. Our findings have practical importance for studies using mouse skin as a model for carcinogenesis, intracutaneous drug delivery and stem cell engineering studies, because they highlight the acute need to differentiate supportive versus inhibitory regions in the host skin.

Mammalian skin contains thousands of hair follicles, each undergoing continuous regenerative cycling. A hair follicle cycles through anagen (growth), catagen (involution) and telogen (resting) phases, and then re-enters the anagen phase. At the base of this cycle is the ability of hair follicle stem cells to briefly exit their quiescent status to generate transient amplifying progeny, but maintain a cluster of stem cells. It is generally believed that a niche microenvironment is important in the control of stem cell homeostasis in various systems<sup>8</sup>. Within a single hair follicle, periodic activation of  $\beta$ -catenin in bulge stem cells is responsible for their cyclic activity<sup>3</sup>. However, how these stem cell activation events are coordinated among neighbouring hairs remains unclear. It is possible that a population of hair follicles

could cycle simultaneously, randomly or in coordinated waves. We recently observed a ‘cyclic alopecia’ phenotype in *Msx2* (homeo box, msh-like 2) null mice, which in essence represents coordinated hair regenerative activity in a population of follicles and is manifest as traversing hair waves<sup>9–11</sup> (Supplementary Fig. 1).

Classical works have documented hair growth waves in rats, mice and other mammals<sup>12,13</sup>. Opinions differ as to whether the hair growth pattern is controlled by local inherent rhythms, systemic factors or both. Because there is a period after anagen during which ‘the systemic stimulus is unable to exert an effect’, the concept of ‘telogen refractivity’ was conceived<sup>14</sup>. A substance, termed ‘chalone’, which can inhibit anagen development, was proposed to explain this phenomenon<sup>15</sup>. However, despite efforts to identify the chalone<sup>16,17</sup>, its molecular nature has remained elusive for the past 50 years.

Intrigued by these dynamic, complex hair growth patterns (Supplementary Fig. 1), we set out to find the underlying molecular mechanisms. A hair-cycle domain is a region of skin that contains a population of hair follicles cycling in coordination. The fact that such domains form implies the existence of signals that serve to spread and stop waves of hair growth. This prompted the suggestion that skin regions in telogen can be in either of the two functional phases: competent telogen, which allows the anagen-re-entry wave to propagate, and refractory telogen, which arrests the wave (Fig. 1a, b). We analysed the cycling behaviour of domains in more than 30 living mice (starting from older than 2 months) for up to 1 year (Supplementary Fig. 1), and consistently found that there is a minimal 28-day-long telogen phase; this was defined as early telogen. After this phase, telogen can either end right away (0 days) or persist for any number of days up to about 60 days. This phase (defined as late telogen) contributes to the apparently highly variable telogen length (Fig. 1c).

This suggests that the first 28 days of telogen are essential for the hair cycle and may represent the refractory phase. To test this idea, we used club-hair (a hair filament that has stopped growing but remains attached in the follicle) plucking, which can induce hair regeneration. We gauged responses by the time required for regeneration to start after hairs are plucked (see Methods). When 50 hairs were plucked from skin in the early telogen phase, a longer time was required for hair growth than when a comparable number of hairs were plucked during late telogen (requiring 42 versus 13 days). When 200 hairs were plucked, the time required for hairs to re-grow became shorter but still differed between early and late telogen (28 versus 9 days; Fig. 1f and Supplementary Fig. 2), so anagen re-entry is faster when 200 hairs were plucked versus 50 hairs. Thus, the functional status of a particular skin region can be determined by the hair plucking/regeneration assay. In the follicles we studied, early (up to 28 days)

<sup>1</sup>Department of Pathology, Keck School of Medicine, University of Southern California, Los Angeles, California 90033, USA. <sup>2</sup>Centre for Mathematical Biology, Mathematical Institute, 24–29 St Giles’, Oxford, OX1 3LB UK. <sup>3</sup>Oxford Centre for Integrative Systems Biology, Department of Biochemistry, South Parks Road, Oxford OX1 3QU, UK. <sup>4</sup>Department of Biochemistry and Molecular Biology, Keck School of Medicine, University of Southern California, Los Angeles, California 90089, USA.

and late (after 28 days) telogen periods correlate well with refractory and competent telogen phases, respectively.

If the refractory and competent states of hair-cycle domains are transient, then offsetting the timing of hair cycling in a localized

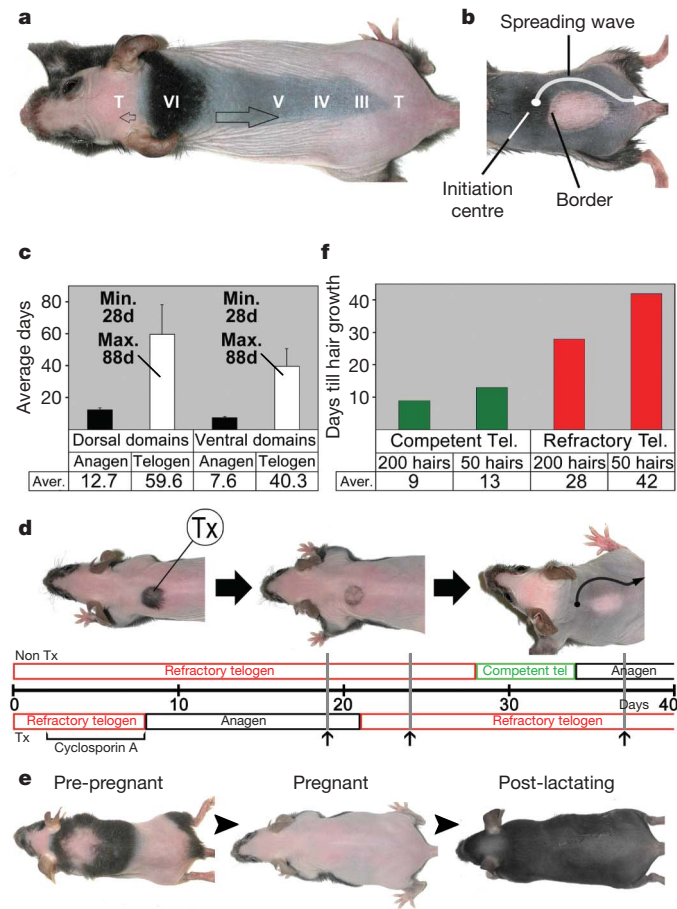


**Figure 1 | Defining refractory and competent telogen.** **a**, Propagation (blank arrows) of hair regenerative waves is seen in *Msx2*-null mice (also see Supplementary Fig. 1). Similar patterns can be seen in normal black mice after hair clipping. Roman characters, anagen stages; T, telogen. **b**, Under physiological conditions, some domains can become refractory to the spreading wave (white arrow). **c**, Normal telogen timing in C57BL/6J mice. The durations of anagen and telogen were measured in 22 hair-cycle domains from dorsal and ventral skin. Error bars represent standard deviation;  $n = 18, 22, 28$  and  $30$ , from left to the right. Min. and Max. represent the range of values, whereas numbers at the bottom represent average (Aver.) number of days. **d**, Experimental induction of refractory telogen with cyclosporine A. The  $x$  coordinate represents the timescale (in days) when experiments began in the early telogen of the non-treated skin region. Cyclosporine A was applied to a localized region (treated, Tx) during early telogen, and induced new anagen about 8 days later. The surrounding non-treated refractory telogen skin (Non Tx) remained in telogen. When the non-treated skin was at day 19 of telogen, treated Tx skin had already proceeded to the late stage of its induced new anagen (left panel, day 19). When non-treated skin was at day 24 of telogen, the cyclosporine-treated region had finished its induced new anagen phase and had entered new telogen (middle panel, day 24). Soon, the non-treated skin progressed into competent telogen. At day 34, the non-Tx region entered its natural anagen. The regenerative wave spread but could not enter the Tx region because it was still in its refractory telogen period (right panel, day 37). Black, anagen; green, competent telogen; red, refractory telogen. **e**, In female mice, multiple hair-cycle domains were reset into one after pregnancy/lactation. Arrowheads, time sequence. **f**, Delayed response to plucking during refractory telogen. Tel., telogen. Hair plucking/regeneration was used to gauge the competent and refractory telogen status ( $n = 16$ ). The minimum time (shown in days) represents the time required for new pigmented hair filaments to be visible. This time is shorter when more hairs were plucked or when the same number of hairs was plucked in the competent period.

region should lead to the formation of new hair-cycle domains. We tested this by local application of cyclosporine A (a powerful anagen-inducing agent that can overcome refractory telogen<sup>18</sup>) to a skin region about 10 mm in diameter that was in telogen day 1. Eight days later, the treated region was in the induced new anagen whereas the surrounding skin continued its progression through refractory telogen. Soon after the treated region completed anagen and re-entered early (new) telogen, the surrounding skin had progressed into late (competent) telogen. When a new hair growth wave approached, it propagated without obstruction over the untreated competent skin, but met resistance in the treated refractory region, thus forming a new hair-cycle domain (Fig. 1d).

Hair-cycle domains are different from regionally specific domains established in development (for example, footpad versus dorsal paw). The exact domain boundaries can shift from cycle to cycle and the domain patterns become more complex as the mouse matures<sup>13</sup> (Supplementary Fig. 1). These complex hair-cycle domains can be affected by systemic factors. For example, during pregnancy and lactation, female mouse hairs that enter telogen are unable to re-enter anagen. Thus, multiple hair-cycle domains are reset into one single domain after pregnancy and lactation<sup>19</sup> (Fig. 1e). Oestrogen and prolactin have been implicated in inhibition of anagen initiation (Supplementary Information).

We wanted to know the molecular mechanisms that constitute this refractoriness. Using *in situ* hybridization and several *lacZ* reporter mice (including *Bmp4-lacZ*, *Nog-lacZ* and the TOPGAL reporter), we searched for cyclic molecular expressions that correlate with refractory and competent telogen. In longitudinal sections of a hair-cycle domain, the hair wave is 'frozen in time' and successive temporal hair-cycle stages are laid out in a spatial order<sup>11</sup>, thus facilitating molecular analyses. We observed canonical WNT signalling and *Msx2*, amongst others, to be expressed in different hair follicle compartments and to fluctuate with hair cycling, as reported (Supplementary Fig. 9). Unexpectedly, we observed the expression dynamics of interfollicular *Bmp2* to be out of phase with that of WNT signalling (Fig. 2a, b, and Supplementary Fig. 5a–e). *Bmp2* expression was absent in early anagen and gradually intensified to reach a peak level in anagen V–VI. *Bmp2* expression remained high in early telogen, but became absent in late telogen (Fig. 2a, b and Supplementary Fig. 5c–e, g). *Bmp4* exhibited similar on and off expression dynamics, as shown by semi-quantitative PCR with reverse transcription, *in situ* hybridization (Fig. 2c, d) and *Bmp4-lacZ* expression (Supplementary Fig. 3). In contrast, *Nog-lacZ* expression showed that on and off dynamics of mesenchymal *Nog* (including dermal papilla and dermal sheath; Supplementary Fig. 4)<sup>17,20</sup> coincides with the hair-cycle rhythm. Because BMP activity can be modulated by multiple factors (different ligands, antagonists and receptors), we measured BMP signalling output by pSMAD (phospho SMAD) 1/5/8 immunostaining; this showed that SMAD 1/5/8 is activated in refractory and is absent in competent telogen hair follicles (Fig. 2e and Supplementary Fig. 6).

We noted that the ability to propagate anagen induction is limited to early anagen follicles. A wave front is halted when it faces a refractory telogen region. By the time this refractory telogen region progresses into competent telogen, the previously propagating anagen follicles have progressed into late anagen and propagation does not resume (Supplementary Fig. 5c, d). Although the surrounding environment is now competent, late anagen follicles are unable to propagate. In this way, the traditional anagen period can be divided into early (anagen I–IV) propagating and late (anagen V, VI) autonomous anagen, with low and high expression of both *Bmp2* and *Bmp4*, respectively, in these phases (Fig. 2a, b and Supplementary Figs 3 and 5). We summarize the rhythms of marker gene expression in Fig. 2g and Supplementary Fig. 10.

Where are the BMP-producing cells? Most of the periodically expressed *Bmp2* transcripts are produced by subcutaneous adipocytes, as judged by double-staining with Sudan Red (Fig. 2f).

Periodic expression of *Bmp4* is seen in the intrafollicular epithelium, secondary hair germ cells, dermal papilla and adjacent extra-follicular dermal fibroblasts (Supplementary Fig. 4). Collectively, we define the extrafollicular sources of periodic *Bmp2* and *Bmp4* expression as the dermal macroenvironment. The macroenvironmental BMPs may have a large additive effect on the strength of intrafollicular (microenvironmental) BMP6 and BMP4 signalling<sup>21,22</sup> in regulating the quiescence of pSMAD-positive bulge stem cells, although these mechanisms remain to be investigated. Because the eventual anagen initiation requires activation of WNT/ $\beta$ -catenin<sup>3,4</sup>, there is competitive equilibrium between BMP and WNT signalling<sup>21</sup>. Stem cells have to integrate the multiple signalling inputs from both the microenvironment and the macroenvironment to make the decision.

The first telogen (around postnatal day 19) is very short and new anagen initiates quickly without detectable refractory telogen. Dermis acquires telogen refractivity with maturation and second telogen (postnatal day 45–70; Supplementary Fig. 6b) does have refractory telogen. These findings lead us to hypothesize that: first, in the ‘BMP on’ phase, the macroenvironment prevents microenvironment-based activation of bulge stem cells (by means of

WNT signalling), resulting in refractory telogen; and, second, in the ‘BMP off’ phase, the macroenvironmental block is removed and the threshold for microenvironment-based activation of stem cells is low. This results in competent telogen; hair follicles are free to enter new anagen either by stochastic self-activation or by facilitation by adjacent early anagen follicles. We tested this hypothesis by transgenic perturbation of BMP signalling, skin transplantation and administration of exogenous BMP4.

If BMPs have a causative role in conferring refractory status, we should be able to reduce the period of refractory telogen by down-regulating BMP signalling. We did this by overexpressing *Nog* under the keratin 14 promoter in *Krt14–Nog* mice<sup>23</sup> (named K14-Noggin in ref. 23). The minimal telogen length was reduced to 6 days, and the maximal length was reduced to 11 days (Fig. 3b). As a result, these mice displayed continuous propagation of hair regenerative waves and have highly simplified hair-cycle-domain patterns (Fig. 3a). We further tested the response of *Krt14–Nog* hair follicles to hair plucking. The differences in response we observed in wild-type mice in early versus late telogen were eliminated in *Krt14–Nog* mice. In all cases, plucked *Krt14–Nog* hair follicles required only approximately 6 days to re-enter anagen (Fig. 3c). Recently, the importance of BMP

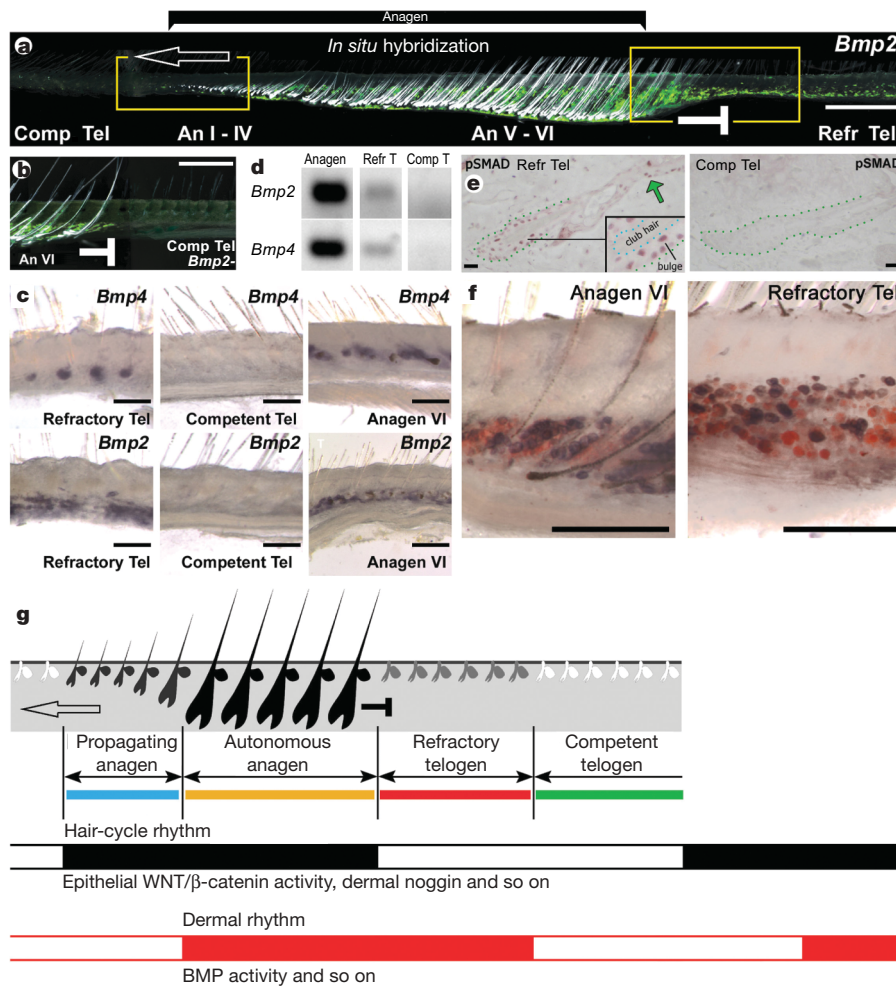


**Figure 2 | Periodic BMP signalling in the dermis and subcutaneous adipose tissue.** **a**, Different temporal stages are spatially laid across the skin strip. The dark-field illumination shows hair follicles (white) and *Bmp2* *in situ* hybridization (green). Note that the beginning and end of the hair cycle and the beginning and end of *Bmp2* *in situ* are out of phase. An, anagen; Comp, competent; Refr, refractory; Tel, telogen. Open arrow, the direction of the spreading waves; stop sign, boundary between anagen and refractory telogen. **b**, When the refractory telogen region becomes competent, anagen VI follicles still do not propagate. **c**, **d**, *Bmp2* and *Bmp4* expressions are

detected by *in situ* and semi-quantitative PCR with reverse transcription. Both methods show that *Bmp2* and *Bmp4* are present in late anagen and refractory telogen, but absent in competent telogen. **e**, pSMAD immunostaining is present in follicular epithelium, including in the bulge area (inset) and adjoining infundibulum (green arrow). **f**, *Bmp2* expression (blue) colocalized within some Sudan-Red-positive adipocytes (red). **g**, Schematic summary of the hair-cycle rhythm (black) and the newly identified dermal rhythm (red). Together, they define four new functional stages. Catagen is omitted for simplification. Scale bars: **a**, 1 mm; **b**, 500  $\mu$ m; **c**, **e**, **f**, 200  $\mu$ m.

activity in suppressing stem cell activity has also been shown by tissue-specific deletion of BMP receptors<sup>21,24</sup>.

The currently held concept of the stem cell microenvironment implies only autonomous regulation: thus, the activation of stem cells depends only on signalling inputs from components intrinsic to the organ (here, the hair follicle itself<sup>3</sup>). To test directly whether the activation of stem cells is also subjected to non-autonomous regulation, we transplanted skin grafts from pigmented *Krt14-Nog* mice onto albino severe combined immunodeficient (SCID) mice. If the control of stem cell activation is intrinsic to the follicles, hair cycling behaviour should remain the same for both donor and host. Instead, we observed donor–host interactions, reflecting a non-autonomous relationship, with the outcome dependent on the size of the transplanted skin graft. When a small graft of *Krt14-Nog* skin (~1 mm) was transplanted, the donor skin remained in telogen for longer and

could respond to an anagen-activating wave originating from the host (Fig. 3e and Supplementary Fig. 7). Thus, we achieved partial functional rescue of *Krt14-Nog* phenotypes. In contrast, when a large skin graft (>10 mm) was transplanted, the graft exhibited a greater degree of autonomous control within itself. Host telogen hair follicles surrounding the graft re-entered anagen (visible as a rim of white hairs) when pigmented donor hairs entered anagen (Fig. 3f) after only 11 days in telogen (versus 28 days), thus providing evidence of a donor effect on the host.

Classical experiments using skin graft transplantation to ask whether hair growth patterns are controlled intrinsically or systemically have produced variable results<sup>14</sup>. We repeated autologous skin transplantation experiments and observed that hair growth patterns are initially intrinsic to the donor but gradually become entrained to the host rhythm after several hair cycles (not shown). Consequently, the discrepancy amongst classical experiments may be due to the size of the graft and the time they chose for readout. At the molecular level, our results demonstrate involvement of the BMP pathway in the non-autonomous interactions among follicle populations. It remains to be investigated whether the process depends on the direct diffusion of BMPs or their antagonists, or whether it is indirectly mediated by other mechanisms<sup>25</sup>.

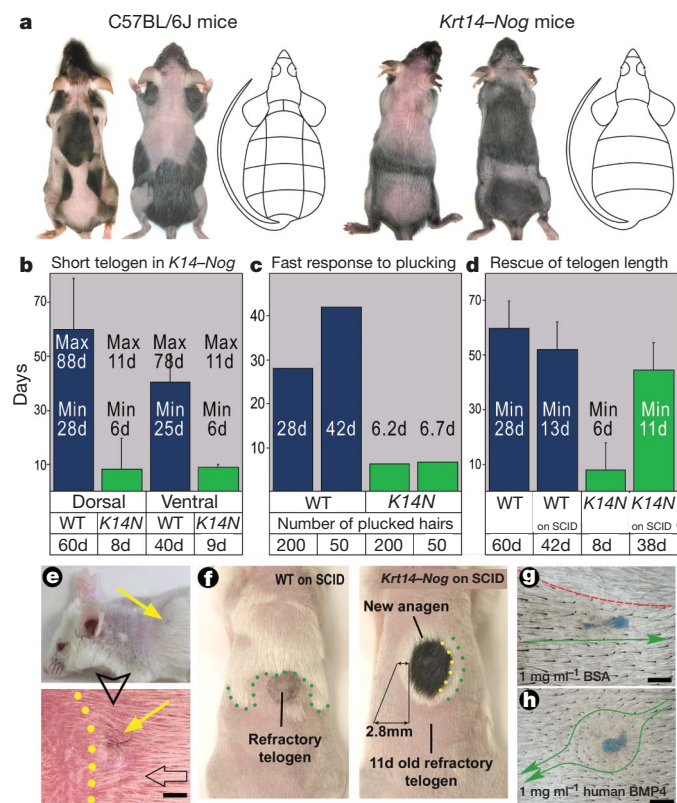


**Figure 3 | Altered hair regenerative wave dynamics in *Krt14-Nog* mice, and non-autonomous interactions with normal cycling host skin after transplantation.** **a**, Control (left) and *Krt14-Nog* (right) mice. Hair-cycle domains in two different stages are shown, together with schematic domain boundaries generated by similar analysis to that used in Supplementary Fig. 1. **b**, Measurements show that both refractory and competent telogen are shortened in *Krt14-Nog* mice (*K14N*, green bars) compared to wild type (WT, blue bars). In **b** and **d**, Min and Max represent range of values, whereas numbers at the bottom represent average number of days. In **c**, however, numbers at the bottom represent numbers of plucked hairs. Error bars, standard deviation;  $n = 71$  for *Nog* mice and  $n = 22-30$  for the control. **c**, Plucking/regenerative response in *Krt14-Nog* (green bars) is about 5 times faster. **d, e**, When a small *Krt14-Nog* skin graft was transplanted into SCID skin, hair growth (**e**) and duration of refractory telogen (**d**) were partially rescued (error bars, standard deviation;  $n > 15$ ). The yellow dotted line represents the anagen wave front. Yellow arrows point at the transplanted *Krt14-Nog* hair follicles. The blank arrow points at the spreading direction of the anagen wave. The blank arrowhead points at the enlarged view of the top panel. **f**, When a large *Krt14-Nog* skin graft (>10 mm) was transplanted, it caused reduction of refractory telogen by inducing a rim of white hair in the host. **g, h**, Human-BMP4-soaked beads caused hair propagation wave (green arrow) to go around them, creating a new telogen domain. Albumin does not have this effect. Red dashed line, domain border. Scale bars: **e, g, h**, 1 mm.

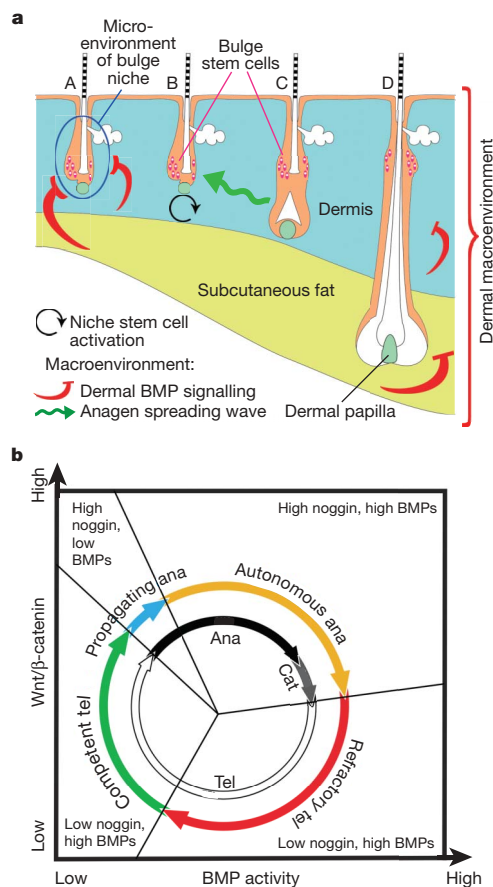


**Figure 4 | Functional phases of the hair cycle.** **a**, Illustration of the bulge niche microenvironment and interfollicular dermal macroenvironment, including dermis, subcutaneous fat and adjacent follicles. Anagen-stimulating (black and green) or -inhibiting (red) activities are depicted with coloured arrows. Follicles are in different stages: A, refractory telogen; B, competent telogen; C, propagating anagen; and D, autonomous anagen follicles. Blue circle in A, intrafollicular microenvironment; colour-coded similar to panel **b**. **b**, New functional phases (coloured outer circle) mapped against classical hair-cycle stages (black and white inner circle). On the basis of the growth-inducing ability of the follicles, anagen is divided into propagating (inducing blue) and autonomous (non-inducing, yellow) phases. On the basis of the ability to respond to regenerative signals, telogen is divided into refractory telogen (red) and competent (green) phases.

Finally, we tested whether a direct local delivery of BMP protein can convert competent telogen status to refractory in normal mice. Human-BMP4-soaked beads were implanted into competent telogen skin ahead of an anagen-spreading wave (see Methods<sup>17</sup>). Twelve days later, human BMP4, but not control BSA, prevented the propagation of the wave around the beads (Fig. 3g, h and Supplementary Fig. 8). Thus, the level of BMP activity can indeed explain the functional status (refractory versus competent) of a skin region.

Results here add new dimensions to our understanding of skin biology. First, these findings demonstrate that, in addition to short distance microenvironmental control<sup>17,22</sup>, the activation of stem cells within large groups of hair follicles is subject to long distance macro-environmental control from the surrounding dermis (Fig. 4). This concept is readily applicable to other organs. For example, whereas *Bmp4* is constantly expressed in the mesenchyme of intestinal microvilli, bursts of *Nog* expression in the villi stem cell niche may act transiently to lower BMP signalling, thus allowing stem cells to proliferate for epithelial renewal<sup>26</sup>. Second, extrafollicular periodically expressed *Bmp2* and *Bmp4* seem to fulfil the criteria of the elegant but elusive chalone proposed to explain patterned hair growth<sup>14,15,17</sup>, thus solving a 50-year-old puzzle. Third, the dynamic expression of *Bmp2* in dermal adipocytes suggests a link between two skin organ systems. Because subcutaneous fat, like hairs, has a thermo-regulatory function and leptin is present in the dermal papilla of hair follicles<sup>27</sup>, periodically expressed *Bmp2* may coordinate the function of these two organs in response to the external environment and may have implications for the evolution of integuments<sup>28</sup>. Fourth, the asynchronous cyclic expression of BMPs and  $\beta$ -catenin in the dermis and hair follicle provide a platform for mutual modulations of these 'clocks' in the skin. They also imply that stem cell regeneration is subject to the control of biological rhythms.

Finally, mouse skin has been used extensively as a model in studies of carcinogenesis, intra-cutaneous drug delivery and stem cell biology<sup>29,30</sup>. Such studies are usually designed on the assumption that the skin is a stable and largely uniform medium. Our findings show clearly that this assumption is rarely, if ever, justified.

## METHODS SUMMARY

**Animals.** C57BL/6J, Crl:CD1(ICR), C3H/HeJ and SCID mice were used in this study. *Msx2* null (C.Cg-*Msx2*<sup>tm1Rim</sup>/Mmcd), *Krt14-Nog* (B6.CBA-Tg(*Krt14-Nog*)), *Bmp4-lacZ* (129S-*Bmp4*<sup>lacZneo</sup>), *Nog-lacZ* (129S-*Nog*<sup>tm1Amc</sup>/J) and TOPGAL (STOCK Tg(*Fos-lacZ*)34Eful) transgenic mice were also used.

**Hair-cycle observation.** Progression of hair growth patterns was monitored in mice for various intervals of time, up to 1 year. Hair clipping was selected over plucking or shaving to avoid wounding that can potentially interfere with normal hair growth<sup>13,15</sup>.

**Animal procedures.** All procedures were performed on anaesthetized animals with protocols approved by USC vivaria. For skin transplantation, surgical procedures were performed when both donor and recipient skins were in early telogen. This was done to ensure that wounded skin is healed by the beginning of the next anagen phase and that the affect of wound healing on the hair cycle is minimal. SCID mice were used as recipients.

**Histology and detection of molecular expressions.** Tissues were collected, fixed and processed for histology as described<sup>13,22</sup>.

**Full Methods** and any associated references are available in the online version of the paper at [www.nature.com/nature](http://www.nature.com/nature).

Received 9 July; accepted 7 November 2007.

1. Stenn, K. S. & Paus, R. Controls of hair follicle cycling. *Physiol. Rev.* **81**, 449–494 (2001).
2. Morris, R. J. *et al.* Capturing and profiling adult hair follicle stem cells. *Nature Biotechnol.* **22**, 411–417 (2004).
3. Fuchs, E., Tumber, T. & Guasch, G. Socializing with the neighbors: stem cells and their niche. *Cell* **116**, 769–778 (2004).
4. Huelsken, J., Vogel, R., Erdmann, B., Cotsarelis, G. & Birchmeier, W.  $\beta$ -Catenin controls hair follicle morphogenesis and stem cell differentiation in the skin. *Cell* **105**, 533–545 (2001).

5. Reddy, S. *et al.* Characterization of Wnt gene expression in developing and postnatal hair follicles and identification of Wnt5a as a target of Sonic hedgehog in hair follicle morphogenesis. *Mech. Dev.* **107**, 69–82 (2001).
6. Lo Celso, C., Prowse, D. M. & Watt, F. M. Transient activation of  $\beta$ -catenin signalling in adult mouse epidermis is sufficient to induce new hair follicles but continuous activation is required to maintain hair follicle tumours. *Development* **131**, 1787–1799 (2004).
7. Lowry, W. E. *et al.* Defining the impact of  $\beta$ -catenin/Tcf transactivation on epithelial stem cells. *Genes Dev.* **19**, 1596–1611 (2005).
8. Moore, K. A. & Lemischka, I. R. Stem cells and their niches. *Science* **311**, 1880–1885 (2006).
9. Ma, L. *et al.* 'Cyclic alopecia' in *Msx2* mutants: defects in hair cycling and hair shaft differentiation. *Development* **130**, 379–389 (2003).
10. Militzer, K. Hair growth pattern in nude mice. *Cell. Tiss. Org.* **168**, 285–294 (2001).
11. Suzuki, N., Hirata, M. & Kondo, S. Traveling stripes on the skin of a mutant mouse. *Proc. Natl Acad. Sci. USA* **100**, 9680–9685 (2003).
12. Durward, A. & Rudall, K. M. Studies on hair growth in the rat. *J. Anat.* **83**, 325–335 (1949).
13. Plikus, M. V. & Chuong, C. M. Complex hair cycle domain patterns and regenerative hair waves in living rodents. *J. Invest. Dermatol.* (in the press) (2007).
14. Ebling, F. J. & Johnson, E. Systemic influence on activity of hair follicles in skin homografts. *J. Embryol. Exp. Morphol.* **9**, 285–293 (1961).
15. Chase, H. Growth of the hair. *Physiol. Rev.* **34**, 113–126 (1954).
16. Paus, R., Stenn, K. S. & Link, R. E. Telogen skin contains an inhibitor of hair growth. *Br. J. Dermatol.* **122**, 777–784 (1990).
17. Botchkarev, V. A. *et al.* Noggin is required for induction of the hair follicle growth phase in postnatal skin. *FASEB J.* **15**, 2205–2214 (2001).
18. Maurer, M., Handjiski, B. & Paus, R. Hair growth modulation by topical immunophilin ligands: induction of anagen, inhibition of massive catagen development, and relative protection from chemotherapy-induced alopecia. *Am. J. Pathol.* **150**, 1433–1441 (1997).
19. Johnson, E. Quantitative studies of hair growth in the albino rat. II. The effect of sex hormones. *J. Endocrinol.* **16**, 351–359 (1958).
20. Botchkarev, V. A. *et al.* Noggin is a mesenchymally derived stimulator of hair-follicle induction. *Nature Cell Biol.* **1**, 158–164 (1999).
21. Kobiak, K., Stokes, N., de la Cruz, J., Polak, L. & Fuchs, E. Loss of a quiescent niche but not follicle stem cells in the absence of bone morphogenetic protein signaling. *Proc. Natl Acad. Sci. USA* **104**, 10063–10068 (2007).
22. Blanpain, C., Lowry, W. E., Geoghegan, A., Polak, L. & Fuchs, E. Self-renewal, multipotency, and the existence of two cell populations within an epithelial stem cell niche. *Cell* **118**, 635–648 (2004).
23. Plikus, M. *et al.* Morpho-regulation of ectodermal organs: integument pathology and phenotypic variations in K14-Noggin engineered mice through modulation of bone morphogenetic protein pathway. *Am. J. Pathol.* **164**, 1099–1114 (2004).
24. Zhang, J. *et al.* Bone morphogenetic protein signaling inhibits hair follicle anagen induction by restricting epithelial stem/progenitor cell activation and expansion. *Stem Cells* **24**, 2826–2839 (2006).
25. Oro, A. E. & Higgins, K. Hair cycle regulation of Hedgehog signal reception. *Dev. Biol.* **255**, 238–248 (2003).
26. He, X. C. *et al.* BMP signaling inhibits intestinal stem cell self-renewal through suppression of Wnt- $\beta$ -catenin signaling. *Nature Genet.* **36**, 1117–1121 (2004).
27. Iguchi, M., Aiba, S., Yoshino, Y. & Tagami, H. Human follicular papilla cells carry out nonadipose tissue production of leptin. *J. Invest. Dermatol.* **117**, 1349–1356 (2001).
28. Wu, P. *et al.* *Evo-Devo* of amniote integuments and appendages. *Int. J. Dev. Biol.* **48**, 249–270 (2004).
29. Sausville, E. A. & Burger, A. M. Contributions of human tumor xenografts to anticancer drug development. *Cancer Res.* **66**, 3351–3354 (2006).
30. Zheng, Y. *et al.* Organogenesis from dissociated cells: generation of mature cycling hair follicles from skin-derived cells. *J. Invest. Dermatol.* **124**, 867–876 (2005).

**Supplementary Information** is linked to the online version of the paper at [www.nature.com/nature](http://www.nature.com/nature).

**Acknowledgements** We thank V. Botchkarev, G. Cotsarelis, B. Morgan, R. Paus, J. Sundberg and R. Widelitz for discussions. We are grateful to B. Hogan, R. Harland and S. Bellusci for providing transgenic mice. This work is supported by Grants from NIAMS and NIA from the NIH, USA, to C.-M.C. M.V.P. is a postdoctoral scholar of the California Institute of Regenerative Medicine. R.E.B. is supported by a Research Councils UK Fellowship and a Microsoft European Postdoctoral Research Fellowship.

**Author Contributions** M.V.P. and C.-M.C. designed the experiment and analysed results together. M.V.P. did major bench work and observations. J.A.M. and D.d.I.C. helped with some bench work. R.E.B. and P.K.M. helped to develop the model. R.M. helped by providing mice and discussing the results.

**Author Information** Reprints and permissions information is available at [www.nature.com/reprints](http://www.nature.com/reprints). Correspondence and requests for materials should be addressed to C.-M.C. ([cmchuong@usc.edu](mailto:cmchuong@usc.edu)).

## METHODS

**Choosing early versus late telogen skin.** To choose early versus late telogen skin in living mice, we used the following protocol.

First, an area on the adult mouse skin where hairs appeared to be growing was chosen. The use of pigmented mice made it easier to distinguish these phases. Hairs were clipped (not plucked) near the skin surface. Anagen-phase skin contains pigment in the proximal hair follicles. This determination can be aided by observing the skin under a dissection microscope, especially when the skin is wet with saline solution to make it appear transparent. These mice were monitored daily, and the day on which skin pigmentation ceased was recorded. This coincides with the anagen/catagen junction. We then waited for an additional 5 days to ensure that skins are in early telogen, giving us early telogen skin to work with. Alternatively, we waited for at least 40 days (well over 4 weeks) after the anagen/catagen junction for late telogen skin to develop, giving us late telogen skin to work with.

**Scoring the plucking experiments.** Hairs were plucked from the early or late telogen region. After plucking, each plucked spot was monitored daily under a dissection microscope. We were able to detect new anagen skin on living mice without having to biopsy or kill the mice for histological specimens. We then looked for changes in pigmentation since the start of melanogenesis in anagen III. Pigmented hairs can be spotted under a dissection microscope before the new hair fibres reach the skin surface. Thus, we were able to record non-invasively the appearance of anagen III hair follicles (when we spotted black hairs under the skin surface). Approximately, this corresponds to the second day of new anagen. It takes another day for the new hair fibre to reach the skin surface. Thus, we were also able to record non-invasively day-3 anagen follicles when the new hair filaments reach above the skin surface.

Because the changes in skin pigmentation are not easily visible, we used the appearance of new hair filaments above the skin surface as the criteria for scoring hair-plucking experiments. Therefore, the results shown in Fig. 1f indicate that it takes approximately 9 days to observe the appearance of day-3 anagen follicles. The extra time includes the period required for the follicle to heal and to get ready to enter anagen.

**Protein administration experiment.** Intracutaneous administration of exogenous protein was performed as follows. Affinity chromatography Affi-gel blue gel beads were obtained from Biorad. Beads were washed in  $1\times$  PBS, followed by drying. The beads were then re-suspended in  $5\ \mu\text{l}$  protein solution, either control (BSA  $1\ \text{mg}\ \text{ml}^{-1}$ ) or experimental (human BMP4  $1\ \text{mg}\ \text{ml}^{-1}$ ), at  $4\ ^\circ\text{C}$  for 30 min. Recombinant human BMP4 protein was obtained from R&D Systems. Reconstitution of the protein was performed in  $4\ \text{mM}$  HCl in  $0.2\%$  BSA as per the manufacturer's guidelines. Approximately 100 beads were introduced to the competent telogen skin of adult mice by means of a single puncture wound to the skin made by a 30 g syringe (insulin syringe). To replenish proteins, subsequent doses of  $1.5\ \mu\text{l}$  protein solution were microinjected to the site of the bead implantation every 24 h by means of a glass micro-needle until the tissue was harvested. After we noted the anagen-spreading wave pass beyond the bead implantation sites (1 week in the case of Fig. 3g, h), we collected the skin and inverted it for photography. This allows the study of the anagen-wave-spreading dynamics around the control and human BMP4 beads.